IChemE

0263–8762/99/$10.00+0.00

Trans IChemE, Vol 77, Part A, October 1999

CFD SIMULATIONS OF SIEVE TRAY HYDRODYNAMICS

R. KRISHNA (FELLOW)*, J. M. VAN BATEN*, J. ELLENBERGER*, A. P. HIGLER*† and R. TAYLOR†

**Department of Chemical Engineering, University of Amsterdam, The Netherlands*
†Department of Chemical Engineering, Clarkson University, Potsdam, New York, USA

A Computational Fluid Dynamics (CFD) model is developed for describing the hydrodynamics of sieve trays. The gas and liquid phases are modelled in the Eulerian framework as two interpenetrating phases. The interphase momentum exchange (drag) coefficient is estimated using the Bennett *et al.* correlation as a basis. Several three-dimensional transient simulations were carried out for a rectangular tray (5 mm holes, 0.22 m× 0.39 m cross section) with varying superficial gas velocity, weir height and liquid weir loads. The simulations were carried out using a commercial code CFX 4.2 of AEA Technology, Harwell, UK and run on a Silicon Graphics Power Challenge workstation with six R10000 200 MHz processors used in parallel. The clear liquid height determined from these simulations is in reasonable agreement with experimental measurements carried out for air-water in a rectangular tray of the same dimensions.

It is concluded that CFD can be a powerful tool for sieve tray design.

Keywords: computational fluid dynamics; sieve trays; clear liquid height; froth height; froth density

INTRODUCTION

The description of the hydrodynamics of sieve trays is of great importance in industrial practice. For a given set of operating conditions (gas and liquid loads), tray geometry (column diameter, weir height, weir length, diameter of holes, fractional hole area, active bubbling area, downcomer area) and system properties, it is required to predict the flow regime prevailing on the tray, liquid hold-up, clear liquid height, froth density, interfacial area, pressure drop, liquid entrainment, gas and liquid phase residence time distributions and the mass transfer coefficients in either fluid phase. There are excellent surveys of the published literature in this area (Kister[1], Lockett[2], Zuiderweg[3]). Published literature correlations are largely empirical in nature.

In recent years there has been considerable academic and industrial interest in the use of computational fluid dynamics (CFD) to model two-phase flows in process equipment. The volume-of-fluid (VOF) technique can be used for a priori determination of the morphology and rise characteristics of single bubbles rising in a liquid (Krishna and van Baten[4]). Considerable progress has been made in CFD modelling of bubbling gas-solid fluidized beds and bubble columns. CFD modelling of fluidized beds usually adopts the Eulerian framework for both the dilute (bubble) and dense phases (emulsion) and makes use of the granular theory to calculate the dense phase rheological parameters (Bogere[5], Boemer *et al.*[6], Ding and Gidaspow[7], Fan and Zhu[8], Ferschneider and Mège[9], Gidaspow[10], Jenkins and Savage[11], Kuipers *et al.*[12], Syamlal and O'Brien[13], van Wachem *et al.*[14,15]). Discrete particle Lagrangian simulations of the particle phases have also been attempted (Hoomans *et al.*[16]). The use of CFD models for gas-liquid bubble columns has also evoked considerable interest in recent years and both Euler-Euler and Euler-Lagrange frameworks have been employed for the description of the gas and liquid phases (Boisson and Malin[17], Delnoij *et al.*[18], Devanathan *et al.*[19], Grevskott *et al.*[20], Grienberger and Hofmann[21], Jakobsen[22], Krishna *et al.*[23], Kumar *et al.*[24], Lapin and Lübbert[25], Lin *et al.*[26], Sokolichin *et al.*[27,28], Torvik and Svendsen[29]). A recent review (Jakobsen *et al.*[30]) analyses the various modelling aspects involved for vertical bubble driven flows.

There have been two recent attempts to model tray hydrodynamics using CFD (Fischer and Quarini[31], Yu *et al.*[32]). Yu *et al.*[32] attempt to model the two-phase flow behaviour using a two-dimensional model, focusing on the description of the hydrodynamics along the liquid flow path, ignoring the variations in the direction of gas flow along the height of the dispersion. Fischer and Quarini[31] have attempted to describe the 3-D transient vapour-liquid hydrodynamics. An important key assumption made in the simulations of Fischer and Quarini[31] concerns the interphase momentum exchange (drag) coefficient; these authors assumed a constant drag coefficient of 0.44, which is appropriate for uniform bubbly flow. This drag coefficient is not appropriate to describe the hydrodynamics of trays operating in either the froth or spray regimes.

In this paper a three-dimensional transient CFD model is developed, within the two-phase Eulerian framework, for hydrodynamics of a rectangular tray. The required interphase momentum exchange coefficient is estimated on the basis of the correlation of Bennett *et al.*[33] for the liquid hold-up. Simulations have been carried out with varying superficial gas velocity, liquid weir loads and weir heights and the results compared with experimental data generated for the air-water system. The objective of this work is examine the extent to which CFD models can be used as a design tool in industrial practice.

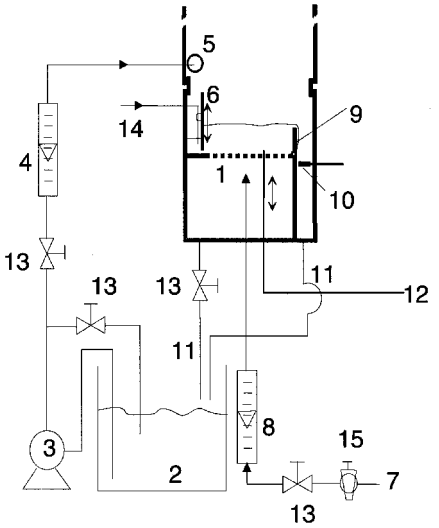

Figure 1. Schematic of experimental set-up to measure hydrodynamics of rectangular sieve tray. 1. Sieve plate; 2. storage tank for liquid; 3. liquid pump; 4. liquid flowmeter; 5. liquid inlet tube; 6. downcomer (adjustable in vertical direction); 7. gas supply; 8. gas flowmeter; 9. weir (exchangeable); 10. conductivity cell for residence time distribution measurements, 11. liquid outlet; 12. liquid filled stainless steel tube connected to a pressure sensor; 13. Valve; 14. tracer injection; 15. quick shut-off valve.

EXPERIMENTAL

The experimental set-up, shown in Figure 1, consists of a rectangular sieve tray and ancillary gas and liquid distribution devices. The sieve tray geometry used in the experiments is shown in Figure 2 and consists of a total of 276 holes of 5 mm diameter (fractional hole area on tray is 0.0627). A calibrated rotameter (8) is used to control the gas flow rate (7). The gas enters the sieve tray trough a 0.025 m diameter copper tube, which has a cap on top to ensure uniform outflow of gas. The superficial gas velocity U_G used in the experiments ranged from 0.5 to 1.2 m s^{-1}. The liquid from the storage tank (2) is fed to the downcomer (6) by means of a centrifugal pump (3). The liquid flow rate is measured by a calibrated liquid flowmeter (4). The liquid loads, per weir length, Q_L/W, ranged from 4×10^{-4} to 12×10^{-4} m^3 s^{-1} m^{-1}. Various weir heights, H_w of 60, 80, 90 and 100 mm were used in the experiments. The liquid inlet tube (5) with an inner diameter of 15 mm is placed above the downcomer (6) and distributes the liquid uniformly over the downcomer cross section through seven equidistant holes of 2 mm diameter.

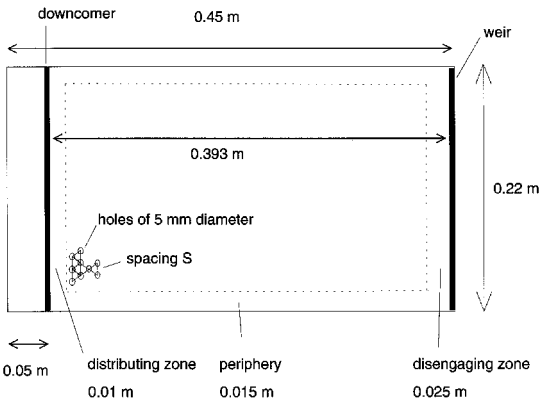

Figure 2. Top view of the geometry of the rectangular sieve tray used in the experiments.

For a specified set of operating conditions, the dispersion height h_{disp} is read from the graduated scale attached to the side of the tray. To measure the clear liquid height, h_{cl}, the gas inlet and liquid inlet are simultaneously, and instantly, switched off and the liquid on the tray is allowed to drain to the container beneath. Measurement of the volume of the liquid thus collected allows determination of the clear liquid height.

Further details of the experimental set up, including photographs of the rig, and measurement technique are available on our web site: http://ct-cr4.chem.uva.nl/tray.

CFD MODEL DEVELOPMENT

For either gas (subscript G) or liquid (subscript L) phases in the two-phase dispersion on the tray the volume-averaged mass and momentum conservation equations are given by

$$\frac{\partial(\varepsilon_G\rho_G)}{\partial t} + \nabla\cdot(\rho_G\varepsilon_G\mathbf{u}_G) = 0 \tag{1}$$

$$\frac{\partial(\varepsilon_L\rho_L)}{\partial t} + \nabla\cdot(\rho_L\varepsilon_L\mathbf{u}_L) = 0 \tag{2}$$

$$\frac{\partial(\rho_G\varepsilon_G\mathbf{u}_G)}{\partial t} + \nabla\cdot(\rho_G\varepsilon_G\mathbf{u}_G\mathbf{u}_G - \mu_G\varepsilon_G(\nabla\mathbf{u}_G + (\nabla\mathbf{u}_G)^T)) = -\varepsilon_G\nabla p + \mathbf{M}_{G,L} + \rho_G\varepsilon_G\mathbf{g} \tag{3}$$

$$\frac{\partial(\rho_L\varepsilon_L\mathbf{u}_L)}{\partial t} + \nabla\cdot(\rho_L\varepsilon_L\mathbf{u}_L\mathbf{u}_L - \mu_L\varepsilon_L(\nabla\mathbf{u}_L + (\nabla\mathbf{u}_L)^T)) = -\varepsilon_L\nabla p - \mathbf{M}_{G,L} + \rho_L\varepsilon_L\mathbf{g} \tag{4}$$

where ρ_k, $\mathbf{u}_k$, ε_k and μ_k represent, respectively, the macroscopic density, velocity, volume fraction and viscosity of the kth phase, p is the pressure, $\mathbf{M}_{G,L}$, the interphase momentum exchange between and liquid phases and $\mathbf{g}$ is the gravitational force. The gas and liquid phases share the same pressure field, $p_G = p_L$. For the continuous, liquid, phase, the turbulent contribution to the stress tensor is evaluated by means of $k-\varepsilon$ model, using standard single phase parameters $C_\mu = 0.09$, $C_{1\varepsilon} = 1.44$, $C_{1\varepsilon} = 1.92$, $\sigma_k = 1$ and $\sigma_\varepsilon = 1.3$. No turbulence model is used for calculating the velocity fields within the dispersed gas phase.

For gas-liquid bubbly flows the interphase momentum exchange term is

$$\mathbf{M}_{L,G} = \frac{3}{4}\rho_L\frac{\varepsilon_G}{d_G}C_D(\mathbf{u}_G - \mathbf{u}_L)\,|\mathbf{u}_G - \mathbf{u}_L| \tag{9}$$

where C_D is the interphase momentum exchange coefficient or drag coefficient. For the Stokes regime

$$C_D = 24/Re_G; \quad Re_G = \rho_L U_G d_G/\mu_L \tag{10}$$

and for the inertial regime, also known as the turbulent regime

$$C_D = 0.44 \tag{11}$$

which is the relation used by Fischer and Quarini[31]. For the churn-turbulent regime of bubble column operation, Krishna *et al.*[34] estimated the drag coefficient of a swarm of large bubbles using

$$C_D = \frac{4}{3}\frac{\rho_L - \rho_G}{\rho_L}gd_G\frac{1}{V_{slip}^2} \tag{12}$$

where V_{slip} is the slip velocity of the bubble swarm with respect to the liquid

$$V_{slip} = |\mathbf{u}_G - \mathbf{u}_L| \tag{13}$$

Substituting equations (12) and (13) into equation (9) gives

$$\mathbf{M}_{L,G} = \varepsilon_G(\rho_L - \rho_G)g\frac{1}{V_{slip}^2}(\mathbf{u}_G - \mathbf{u}_L)\,|\mathbf{u}_G - \mathbf{u}_L| \tag{14}$$

The slip between gas and liquid can be estimated from superficial gas velocity U_G and the gas hold-up ε_G

$$V_{slip} = U_G/\varepsilon_G \tag{15}$$

In this work the Bennett *et al.*[33] correlation is used to estimate the gas hold-up:

$$\varepsilon_L^B = \exp\left[-12.55\left(u_s\sqrt{\frac{\rho_{gas}}{\rho_{liq}-\rho_{gas}}}\right)^{0.91}\right]; \quad \varepsilon_G^B = 1 - \varepsilon_L^B \tag{16}$$

The interphase momentum exchange term is therefore

$$\mathbf{M}_{L,G} = \varepsilon_G(\rho_L - \rho_G)g\frac{1}{(U_G/\varepsilon_G^B)^2}(\mathbf{u}_G - \mathbf{u}_L)\,|\mathbf{u}_G - \mathbf{u}_L| \tag{17}$$

This formulation, however, gives numerical difficulties during start-up of the tray with fresh liquid because in the freeboard the liquid hold-up is zero. In order to overcome this problem equation (17) is modified as follows

$$\mathbf{M}_{L,G} = \varepsilon_G\varepsilon_L(\rho_L - \rho_G)g\frac{1}{(U_G/\varepsilon_G^B)^2}\frac{1}{\varepsilon_L^B}(\mathbf{u}_G - \mathbf{u}_L)\,|\mathbf{u}_G - \mathbf{u}_L| \tag{18}$$

where the term $1/(U_G/\varepsilon_G^B)^2\ 1/\varepsilon_L^B$ is estimated a priori from the Bennett relation (16). This approach ensures that the average gas hold-up in the gas-liquid dispersion on the froth conforms to experimental data over a wide range of conditions (as measured by Bennett *et al.*[33]). When incorporating equation (18) for the gas-liquid momentum exchange within the momentum balance relations (3) and (4) the local, transient, values of $\mathbf{u}_G$, $\mathbf{u}_L$, ε_G and ε_L are used. A further point to note is that use of equation (18) for the momentum exchange obviates the need for specifying the bubble size; indeed for the range of superficial gas velocities used in our experiments and simulations there are no well defined bubbles. The two-phase Eulerian simulation approach used here only requires that the gas phase be the dispersed phase; this dispersion could consist of either gas bubbles or gas jets, or a combination thereof.

A commercial CFD package CFX 4.2 of AEA Technology, Harwell, UK, was used to solve the equations of continuity and momentum for the two-fluid mixture. This package is a finite volume solver, using body-fitted grids. The grids are non-staggered and all variables are evaluated at the cell centres. An improved version of the Rhie-Chow[35] algorithm is used to calculate the velocity at the cell faces. The pressure-velocity coupling is obtained using the SIMPLEC algorithm (Van Doormal and Raithby[36]). For the convective terms in equations (1)–(4) hybrid differencing was used. A fully implicit backward differencing scheme was used for the time integration.

The dimensions of the computational space are 0.39× 0.12× 0.22 m, as shown in Figure 3. Grid cells of 5 mm size are used in the x-, y- and z- directions. The choice

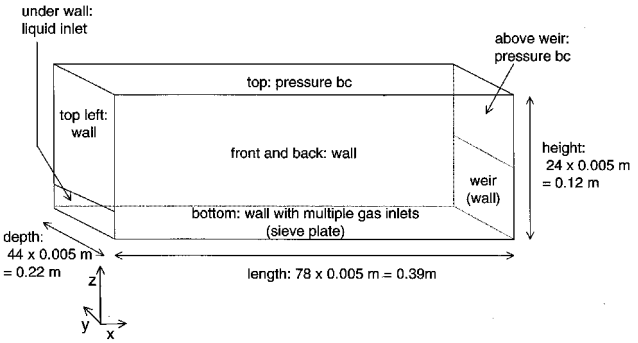

Figure 3. Specification of the computational space used in the CFD simulations.

of the grid size is based on experience gained in the modelling of gas-liquid bubble columns operating in the churn-turbulent regime (Krishna[37]). The chosen grid size of 5 mm is smaller than the smallest grid used in our earlier study (Krishna[37]), where grid convergence was satisfied. The total number of grid cells within the computational space is 78× 24× 44 = 82368. Figure 4 shows the layout of holes at the sieve plate in the bottom of the system. The fractional free-area in the computations is the same as that used in the experiments; however, square holes are used in the simulations rather than circular holes because a rectangular Cartesian coordinate system is used. The use of square holes inside of circular holes does not impact on the simulation results because the Eulerian framework is used for describing either fluid phase. The geometry of the holes would influence the results in VOF simulations, which is used for a priori prediction of bubble dynamics (Krishna and van Baten[4])

Simulations have been performed on a Silicon Graphics Power Challenge with six R10000 processors running in parallel at 200 Mhz. A representative dynamic simulation took about 2 days to attain steady state. From the simulation results, average liquid hold-up as a function of height has been determined. Dispersion height has been defined by the height at which the average liquid hold-up drops below 10 percent. Clear liquid height has been determined by multiplying the average total system liquid hold-up with the height of the system. Average liquid hold-up has been calculated by dividing clear liquid height by dispersion height.

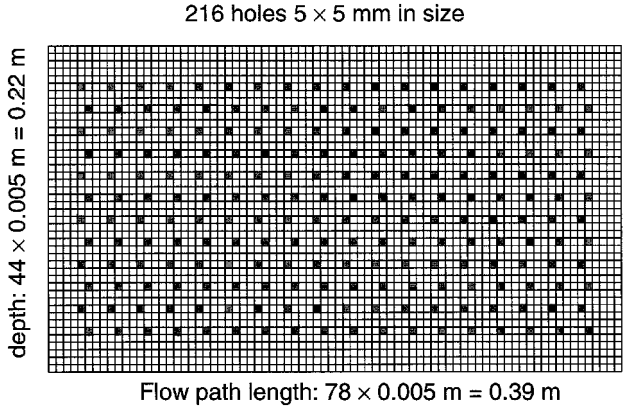

Figure 4. Layout of the sieve plate used in the CFD simulations. The grid size is 5 mm and 216 5 mm square holes are used in the simulations.

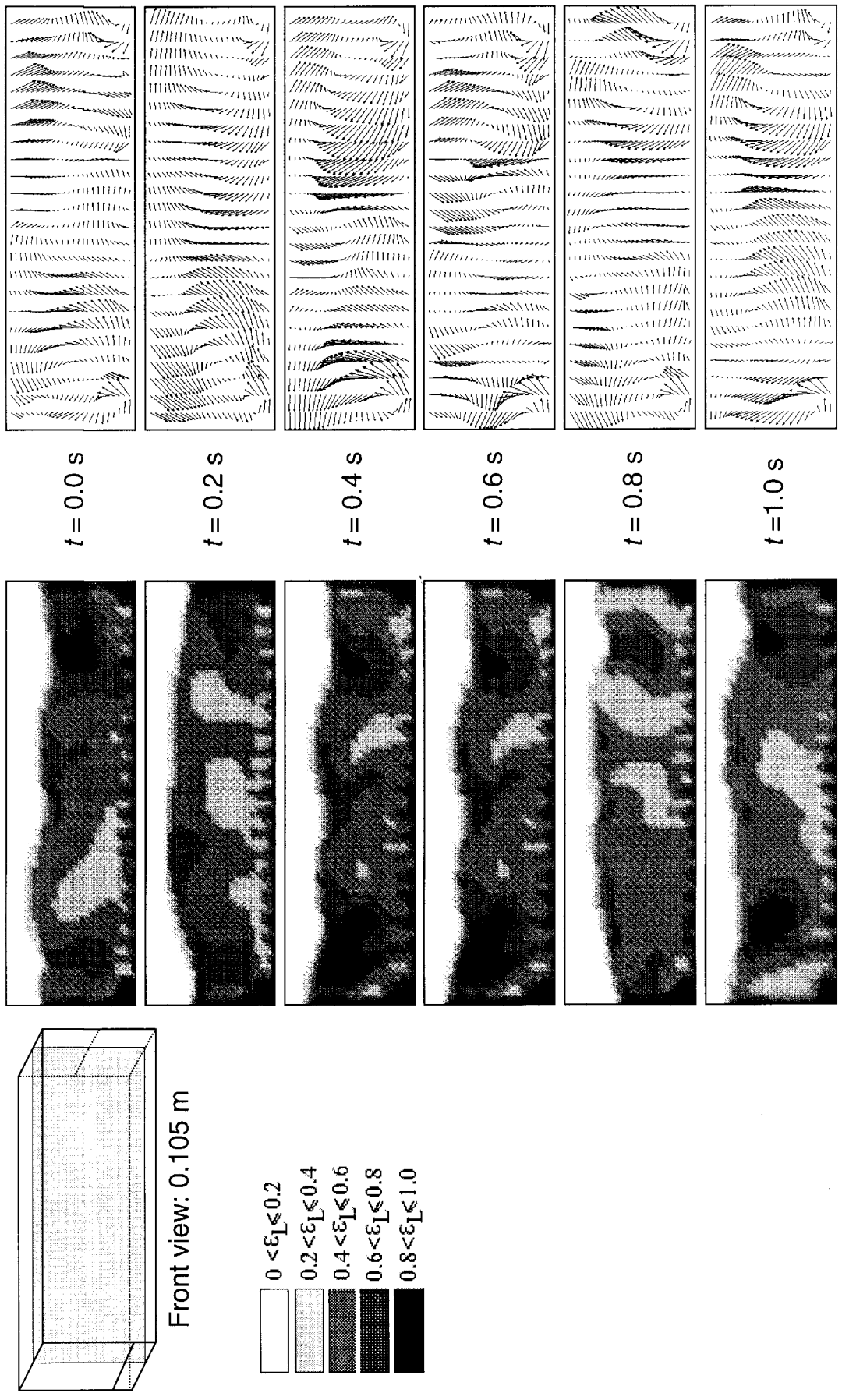

Figure 5. Snapshots of the front view of the Eulerian simulations at a superficial gas velocity, $U_G = 0.7\ \mathrm{m\,s^{-1}}$; weir height $h_w = 80$ mm; liquid weir load $Q_L/W = 8.25\times 10^{-4}\ \mathrm{m^3\,s^{-1}\,m^{-1}}$. An animation of the simulation can be viewed on our web site: http://ct-cr4.chem.uva.nl/trayCFD.

Further details of the computational algorithms used, boundary conditions, including an animation of a typical simulation are available on our web site: http://ct-cr4.chem.uva.nl/trayCFD.

Quasi-steady state values are obtained by running a dynamic simulation until no more changes in the total liquid hold-up in the system are observed for a period large enough to obtain a time average. The largest time step used in the simulations is 2×10^{-3} s. The approach to a quasi-steady state is done by monitoring the liquid liquid in the system. Typically, 3000 time steps are required to attain quasi-steady state conditions. To obtain steady state values of the clear liquid height, presented later in this work, instantaneous results have been averaged over a time period in which the liquid holdup in the system remained practically constant.

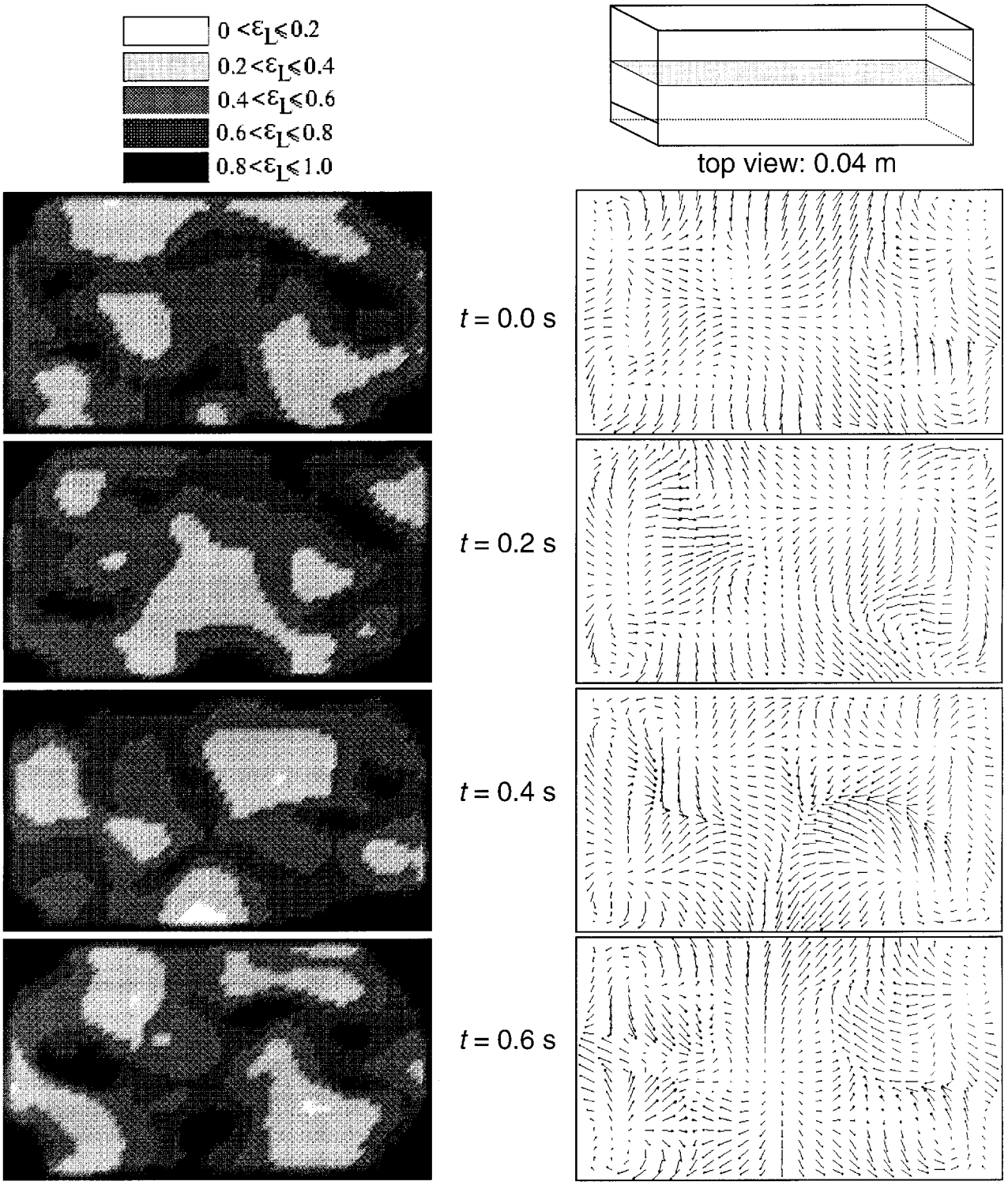

Figure 6. Snapshots of the top view of the Eulerian simulations at a superficial gas velocity, U_G = 0.7 m s^{-1}; weir height h_w = 80 mm; liquid weir load $Q_L/W = 8.25\times 10^{-4}$ m^3 s^{-1} m^{-1}. An animation of the simulation can be viewed on our web site: http://ct-cr4.chem.uva.nl/trayCFD.

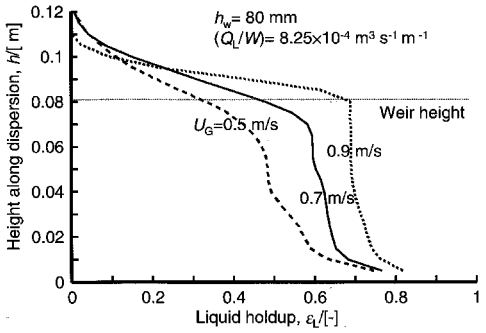

Figure 7. Distribution of liquid hold-up along the height of the dispersion for superficial gas velocities, U_G = 0.5, 0.7 and 0.9 m s^{-1}. Weir height h_w = 80 mm; liquid weir load Q_L/W = 8.25× 10^{-4} m^3 s^{-1} m^{-1}. The values of the hold-up are obtained after averaging along the *x*- and *y*- directions and over a sufficiently long time interval once quasi-steady state conditions are established.

CFD SIMULATIONS VS EXPERIMENTS

Figures 5 and 6 present computational snapshots of the front view and top view of the tray. The existence of liquid circulation cells is apparent, as is the chaotic behaviour of the tray. Figure 7 presents typical simulation results for the variation of the liquid hold-up along the height of the dispersion. The values of the hold-up are obtained after averaging along the x- and y- directions and over a sufficiently long time interval once quasi-steady state conditions are established. The simulated trends in the liquid hold-up with gas velocity U_G are in line with experimental data (e.g. Zuiderweg[3]).

Figure 8 compares the experimental data for the clear liquid height with varying superficial gas velocity with the results from CFD simulations and four typical literature correlations (Bennett *et al.*[33], Colwell[38], Hofhuis and Zuiderweg[39], Stichlmair[40]). The values of the clear liquid height from the simulations are obtained after averaging over a sufficiently long time interval once quasi-steady state conditions are established and determining the cumulative liquid hold-up within the computational space. Figures 9 and 10 compare the experimental data for the clear liquid height with varying liquid weir loads and weir height,

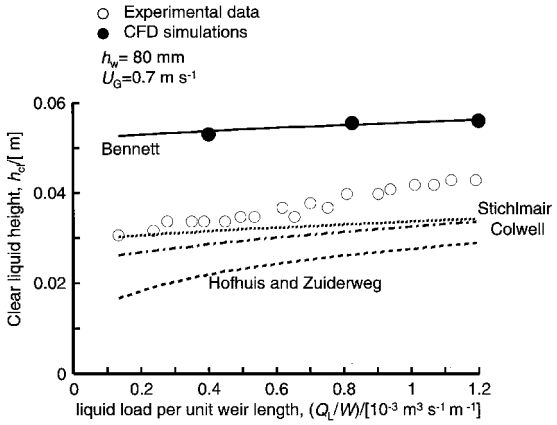

Figure 9. Clear liquid height as a function of the liquid weir load. Comparison of experimental data with literature correlations and CFD simulations. Weir height h_w = 80 mm; Superficial gas velocity U_G = 0.7 m s^{-1}. The values of the clear liquid height from the simulations are obtained after averaging over a sufficiently long time interval once quasi-steady state conditions are established and determining the cumulative liquid hold-up within the computational space.

respectively, with the results from CFD simulations and literature correlations. Of the literature correlations, those of Colwell[38] and Stichlmair[40] agree best with our experimental results. In the present experiments it was found that small amounts of impurities and surface active agents tend to influence the experimental results to a significant extent. The Bennett correlation and our CFD simulations give a good representation of systems which show good coalescence behaviour. If coalescence is suppressed by the presence of impurities, the gas holdup would tend to increase with a concomitant decrease in the clear liquid height. Apparently, the correlations of Colwell, Stichlmair and Hofhuis and Zuiderweg work best for non-coalescing systems. Such systems can be simulated by making the appropriate changes in the slip velocity relation used in equation (18).

In Figure 10 it is noted that the deviation between our CFD simulations and the Bennett correlation for the clear liquid height increases when the weir height increases to

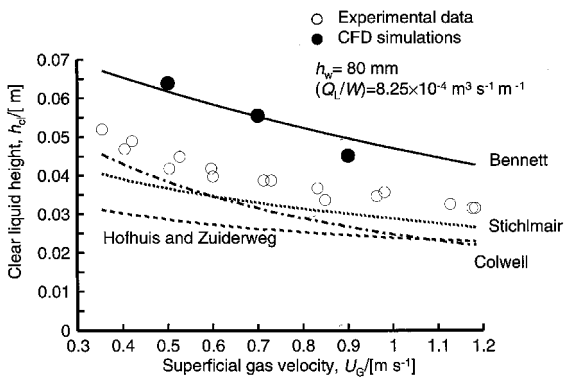

Figure 8. Clear liquid height as a function of the superficial gas velocity. Comparison of experimental data with literature correlations and CFD simulations. Weir height h_w = 80 mm; liquid weir load Q_L/W = 8.25× 10^{-4} m^3 s^{-1} m^{-1}. The values of the clear liquid height from the simulations are obtained after averaging over a sufficiently long time interval once quasi-steady state conditions are established and determining the cumulative liquid hold-up within the computational space.

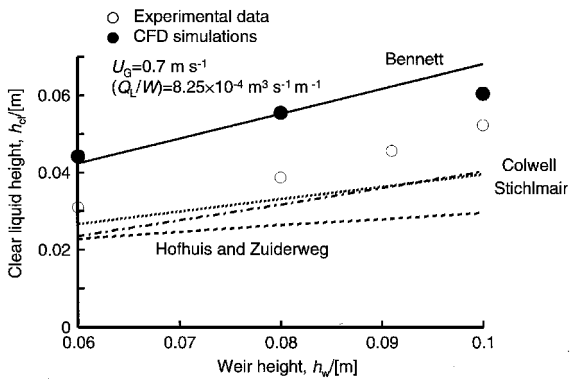

Figure 10. Clear liquid height as a function of the weir height. Comparison of experimental data with literature correlations and CFD simulations. Q_L/W = 8.25× 10^{-4} m^3 s^{-1} m^{-1}; Superficial gas velocity U_G = 0.7 m s^{-1}. The values of the clear liquid height from the simulations are obtained after averaging over a sufficiently long time interval once quasi-steady state conditions are established and determining the cumulative liquid hold-up within the computational space.

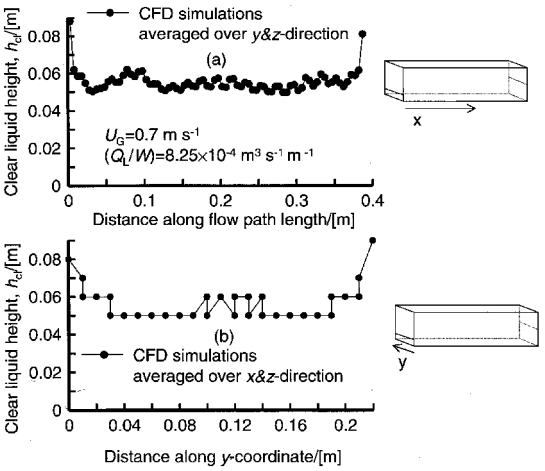

Figure 11. Clear liquid height along the x- and y- directions. Q_L/W = 8.25×10^{-4} m^3 s^{-1} m^{-1}; U_G = 0.7 m s^{-1}; h_w = 80 mm. The values of the clear liquid height from the simulations are obtained after averaging over a sufficiently long time interval once quasi-steady state conditions are established and determining the clear liquid height by averaging over (a) y and z, and (b) over x and z directions respectively.

values larger than 80 mm. The reason for this deviation is because the values of h_w in the experiments of Bennett *et al.* ranged from 0–25 mm. The improved agreement between the CFD simulations and experiments with increasing weir heights, suggests that the assumed drag relations are more applicable to the bubbly froth regime rather than to the spray regime.

In Figures 8, 9 and 10 the clear liquid heights were determined by averaging over the x, y and z directions of the computational space (see Figure 3). For a typical run, with $Q_L/W = 8.25\times 10^{-4}$ m^3 s^{-1} m^{-1}, $U_G = 0.7$ m s^{-1} and h_w = 80 mm, the clear liquid heights in the x- and y- directions are given in Figure 11 (a) and (b). The 'bath-tub' profiles of the clear liquid height are clearly evident.

CONCLUDING REMARKS

A transient three-dimensional CFD model has been developed for tray hydrodynamics. The gas and liquid phases are treated as interpenetrating continuous phases and modelled within the Eulerian framework. The only empirical input to the CFD simulations is the slip velocity between the gas and liquid phases; for this purposes the Bennett[33] correlation was used. The predictions of the clear liquid height and liquid hold-up from the CFD simulations show the right trends with varying superficial gas velocity, liquid weir load and weir height. However, there is a tendency for the CFD simulations to consistently over-predict the clear liquid height for our measurements. The reason for this overprediction is the Bennett correlation for estimation of the slip between the gas and liquid phases; this correlation is appropriate for systems without any coalescence inhibiting impurities or surface active agents.

The important advantage of the CFD simulations is that the influence of tray geometry is automatically taken into account by the code. It is concluded that CFD simulations can be a powerful design and simulation tool.

There is a need for developing more fundamental models for calculation of the interphase momentum exchange between the gas and liquid phases on a tray. Such relations must clearly be dependent on the operating regime of the tray.

NOMENCLATURE

d_G	diameter of gas bubble, m
C_D	drag coefficient, dimensionless
g	acceleration due to gravity, 9.81 m s^{-2}
H	dispersion height, m
$\mathbf{M}$	interphase momentum exchange term, N m^{-3}
p	pressure, N m^{-2}
Q_L	liquid flow rate across tray, m^3 s^{-1}
Re	Reynolds number, dimensionless
t	time, s
$\mathbf{u}$	velocity vector, m s^{-1}
U_G	superficial gas velocity, m s^{-1}
V_{slip}	slip velocity between gas and liquid, m s^{-1}
W	weir length, m
x	coordinate, m
y	coordinate, m
z	coordinate, m

Greek letters

ε	volume fraction of phase, dimensionless
μ	viscosity of phase, Pa s
ρ	density of phases, kg m^{-3}
τ	stress tensor, N m^{-2}

Subscripts

cl	clear liquid
disp	dispersion
G	referring to gas phase
k	index referring to one of the three phases
L	referring to liquid phase
slip	slip

Superscripts

B	from Bennett correlation

REFERENCES

1. Kister, H. Z., 1992, *Distillation Design*, (McGraw-Hill, New York).
2. Lockett, M. J., 1986, *Distillation Tray Fundamentals*, (Cambridge University Press).
3. Zuiderweg, F. J., 1982, Sieve trays. A view on the state of the art, *Chem Eng Sci*, 37: 1441–1464.
4. Krishna, R. and Van Baten, J. M., 1999, Simulating the motion of gas bubbles in a liquid, *Nature*, 398: 208.
5. Bogere, M. N., 1996, A rigorous description of gas-solid fluidized beds, *Chem Eng Sci*, 51: 603–622.
6. Boemer, A., Qi, H., Renz, U., Vasquez and Boysan, F., 1995, Eulerian computation of fluidized bed hydrodynamics—A comparison of physical models. *Proc 13th Int Conf on Fluidized Bed Combustion, Orlando, USA*, pp. 775–787.
7. Ding, J and Gidaspow, D., 1990, A bubbling fluidization model using the kinetic theory of granular flow, *AIChEJ*, 36: 523–538.
8. Fan, L. S. and Zhu, C., 1998, *Principles of Gas-Solid Flows*, (Cambridge University Press, Cambridge).
9. Ferschneider, G. and Mège, P., 1996, Eulerian simulation of dense phase fluidized beds, *Revue de L'Institut Français du Pétrole*, 51: 301–307.
10. Gidaspow, D., 1994, *Multiphase Flow and Fluidization–Continuum and Kinetic Theory Descriptions*, (Academic Press).
11. Jenkins, J. T. and Savage, S. B., 1983, A theory for the rapid flow identical, smooth, nearly elastic spherical particles, *J Fluid Mech*, 130: 187–202.
12. Kuipers, J. A. M., van Duijn, K. J., van Beckum, F. P. H. and Van Swaaij, W. P. M., 1992, A numerical model of gas-fluidized beds, *Chem Eng Sci*, 47: 1913–1924.
13. Syamlal, M. and O'Brien, T. J., 1989, Computer simulation of bubbles in a fluidized bed. *AIChE Symp Series No. 270*, 85: pp. 22–31.
14. Van Wachem, B. G. M., Schouten, J. C., Krishna, R. and Van den Bleek, C. M., 1998, Eulerian simulations of bubbling behaviour in gas-solid fluidized beds, *Comput Chem Eng*, 22: S299–S306.

15. Van Wachem, B. G. M., Schouten, J. C., Krishna, R. and Van den Bleek, C. M., 1999, Validation of the Eulerian simulated dynamic behaviour of gas-solid fluidized beds, *Chem Eng Sci*, 54: 2141–2149.
16. Hoomans, B. P. B., Kuipers, J. A. M., Briels, W. J. and Van Swaaij, W. P. M., 1996, Discrete particle simulation of bubble and slug formation in a two-dimensional gas-fluidized bed: A hard sphere approach, *Chem Eng Sci*, 51: 99–118.
17. Boisson, N. and Malin, M. R., 1996, Numerical prediction of two-phase flow in bubble columns, *Int J Numerical Methods in Fluids*, 23: 1289–1310.
18. Delnoij, E., Lammers, F. A., Kuipers, J. A. M. and Van Swaaij, W. P. M., 1997, Dynamic simulation of dispersed gas-liquid two-phase flow using a discrete bubble model, *Chem Eng Sci*, 52: 1429–1458.
19. Devanathan, N., Dudukovic, M. P., Lapin, A. and Lübbert, A., 1995, Chaotic flow in bubble column reactors, *Chem Eng Sci*, 50: 2661–2667.
20. Grevskott, S., Sannæs, B. H., Dudukovic, M. P., Hjarbo, K. W. and Svendsen, H. F., 1996, Liquid circulation, bubble size distributions, and solids movement in two- and three-phase bubble columns, *Chem Eng Sci*, 51: 1703–1713.
21. Grienberger, J and Hofmann, H., 1992, Investigations and modelling of bubble columns, *Chem Eng Sci*, 47: 2215–2220.
22. Jakobsen, H. A., 1993, On the modelling and simulation of bubble column reactors using a two-fluid model, *Dr Ing Thesis*, (The University of Trondheim, The Norwegian Institute of Technology, Department of Chemical Engineering, Trondheim).
23. Krishna, R., Van Baten, J. M. and Ellenberger, J., 1998, Scale effects in fluidized multiphase reactors, *Powder Technol*, 100: 137–146.
24. Kumar, S., Vanderheyden, W. B., Devanathan, N., Padial, N. T., Dudukovic, M. P. and Kashiwa, B. A., 1995, Numerical simulation and experimental verification of gas-liquid flow in bubble columns, In *Industrial Mixing Fundamentals with Applications, AIChE Symp Series No. 305*, 91: pp. 11–19.
25. Lapin, A. and Lübbert, A., 1994, Numerical simulation of the dynamics of two-phase gas-liquid flows in bubble columns, *Chem Eng Sci*, 49: 3661–3674.
26. Lin, T. J., Reese, J., Hong, T. and Fan, L. S., 1996, Quantitative analysis and computation of two-dimensional bubble columns, *AIChEJ*, 42: 301–318.
27. Sokolichin, A. and Eigenberger, G., 1994, Gas-liquid flow in bubble columns and loop reactors: Part I. Detailed modelling and numerical simulation, *Chem Eng Sci*, 49: 5735–5746.
28. Sokolichin, A., Eigenberger, G., Lapin, A. and Lübbert, A., 1997, Direct numerical simulation of gas-liquid two-phase flows. Euler/Euler versus Euler/Lagrange, *Chem Eng Sci*, 52: 611–626.
29. Torvik, R. and Svendsen, H. F., 1990, Modelling of slurry reactors. A fundamental approach, *Chem Eng Sci*, 45: 2325–2332.
30. Jakobsen, H. A., Sannæs, B. H., Grevskott, S., and Svendsen, H. F., 1997, Modeling of bubble driven vertical flows, *Ind Eng Chem Res*, 36: 4052–4074.
31. Fischer, C. H. and Quarini, G. L., 1998, Three-dimensional heterogeneous modelling of distillation tray hydraulics, Paper presented at the *AIChE annual meeting, 15-20 November 1998, Miami Beach, USA*.
32. Yu, K. T., Yan, X. G., You, X. Y., Liu, F. S. and Liu, C. J., 1998, Computational fluid-dynamics and experimental verification of two-phase two-dimensional flow on a sieve column tray. Paper presented at the *Working Party meeting on Distillation, Absorption and Extraction, EFChE, Cagliari, 5-7 October 1998*.
33. Bennett, D. L., Agrawal, R. and Cook, P. J., 1983, New pressure drop correlation for sieve tray distillation columns, AIChEJ, 29: 434–442.
34. Krishna, R., Urseanu, M. I., Van Baten, J. M. and Ellenberger, J., 1999, Rise velocity of a swarm of large gas bubbles in liquids, *Chem Eng Sci*, 54: 171–183.
35. Rhie, C. M. and Chow, W. L., 1983, Numerical study of the turbulent flow past an airfoil with trailing edge separation, *AIAA Journal*, 21: 1525–1532.
36. Van Doormal, J and Raithby, G. D., 1984, Enhancement of the SIMPLE method for predicting incompressible flows, *Numer Heat Transfer*, 7: 147–163.
37. Krishna, R., Urseanu, M. I., Van Baten, J. M. and Ellenberger, J. 1999, Influence of scale on the hydrodynamics of bubble columns operating in the churn-turbulent regime: Experiments vs Eulerian simulations, *Chem Eng Sci*, 54: 4903–4911.
38. Colwell, C. J., 1979, Clear liquid height and froth densities on sieve trays. *Ind Eng Chem Proc Des Dev*, 20: 298–307.
39. Hofhuis, P. A. M. and Zuiderweg, F. J., 1979, Sieve plates: dispersion density and flow regimes. *IChemE Symp Series No 56*, pp. 2.2/1–2.2/26.
40. Stichlmair, J., 1978, *Grundlagen der Dimensionierung des Gas/Flüssigkeit-Kontaktapparates Bodenkolonne*, Reprotext, (Verlag Chemie, Weinheim).

ACKNOWLEDGEMENT

The Netherlands Foundation for Scientific Research (NWO) is gratefully acknowledged for providing financial assistance to J.M. van Baten.

ADDRESS

Correspondence concerning this paper should be addressed to Professor R. Krishna, Department of Chemical Engineering, University of Amsterdam, Nieuwe Achtergracht 166, 1018 WV Amsterdam, The Netherlands. (E-mail: krishna@chemeng.chem.uva.nl).

The manuscript was received 15 January 1999 and accepted for publication after revision 14 May 1999.